ORIGINAL RESEARCH

Frequent infiltration of S-100 protein+ CCR5+ immature dendritic cells in damaged bile ducts of primary biliary cirrhosis compared to cholangiocellular carcinoma

Hiroko Mitsui[1,2]
Hiroya Ohtake[1]
Rintaro Ohe[1]
Mitsunori Yamakawa[1]

[1]Department of Pathological Diagnostics, [2]Department of Gastroenterology, Yamagata University Faculty of Medicine, Yamagata, Japan

Abstract: Dendritic cells (DCs) are professional antigen presenting cells that initiate immune responses. We evaluated the relationship between DC infiltration, chemokines/chemokine receptors, and bile duct damage in primary biliary cirrhosis (PBC), compared to cases of cholangiocellular carcinoma arising from the bile duct. Immunohistochemistry revealed significantly more S-100 protein+ DCs infiltrating the epithelial layer of bile ducts in PBC than in chronic hepatitis C or control neonatal livers. Furthermore, a higher number of S-100 protein+ DCs, but not fascin+ or DC lysosomal associated membrane protein+ mature DCs, were found in the epithelial layer of the damaged bile ducts of the PBC liver. CC-chemokine receptor (CCR) 5+ immature DCs frequently accumulated in the portal area in PBC. CCR5 mRNA was also detected in liver tissues from PBC patients by reverse transcription polymerase chain reaction. In situ hybridization revealed the expression of macrophage inflammatory protein (MIP)-1α and MIP-1β mRNA in the epithelial cells of damaged bile ducts. However, no CD1a+ immature DCs were found in any of the PBC or chronic hepatitis C specimens or in neonatal liver, whereas they occurred frequently in the cancer nests of cholangiocellular carcinoma, which expressed MIP-3α and were frequently infiltrated by CCR6+ DCs. These results indicate that bile ducts damaged by PBC secrete MIP-1α and MIP-1β, while neoplastic ones secrete MIP-3α. They also suggest that CCR5+ immature DCs attracted by MIP-1α and MIP-1β may play an important role in the pathogenesis of chronic nonsuppurative destructive cholangitis in PBC.

Keywords: chemokines, cholangiocellular carcinoma, chronic nonsuppurative destructive cholangitis, dendritic cell, primary biliary cirrhosis

Introduction

Primary biliary cirrhosis (PBC) is an autoimmune liver disease characterized histologically by progressive destruction of the small intrahepatic bile ducts, known as chronic nonsuppurative destructive cholangitis (CNSDC). Immune reactions involving T-cell-mediated responses to target antigens expressed on the epithelial cells of the intralobular bile ducts and periportal hepatocytes are the key to understanding the pathogenesis of PBC.

Dendritic cells (DCs) are professional antigen presenting cells that function as the sentinels of the immune system in lymphoid and nonlymphoid tissues.[1–3] Immature DCs capture antigens and, after developing into mature DCs, become strong primers of naïve T-cells. DCs are closely involved in the development of chronic persistent inflammation in various autoimmune diseases, including PBC.

Correspondence: Mitsunori Yamakawa
Department of Pathological Diagnostics, Yamagata University Faculty of Medicine, 2-2-2 Iida-Nishi, Yamagata 990-9585, Japan
Tel +81 23 628 5237
Fax +81 23 628 5240
Email myamakaw@med.id.yamagata-u.ac.jp

The migration, differentiation, and activation of DCs are controlled by factors such as adhesion molecules, cytokines, and chemokines. The chemokine family plays an important role in signaling the induction of an immune response by ligating to and activating various receptors expressed on inflammatory cells and DCs.[4–9] Immature DCs express several chemokine receptors, such as CC-chemokine receptor (CCR) 1, CCR2, CCR5, CCR6 and CXC-chemokine receptor (CXCR) 4. In addition to the specific ligands, macrophage inflammatory protein (MIP)-1α/CC ligand (L) 3 can bind to CCR1 and CCR5, MIP-1β/CCL4 can bind to CCR5, MIP-3α/CCL20 can bind to CCR6, monocyte chemotactic protein-4 (MCP-4/CCL13) can bind to CCR2, regulated upon activation, normal T expressed and secreted (RANTES/CCL5) can bind to CCR1 and CCR5, and stromal cell-derived factor-1/CXCL12 can bind to CXCR4.

A few previous studies have revealed that cells expressing relatively DC specific antigens, including S-100 protein, CD1a, CD83, and BDCA-2, localized in liver specimens obtained from patients with PBC.[10–15] Moreover, several chemokines and chemokine receptors have recently been demonstrated to be expressed in certain liver diseases, including PBC.[14–21] However, information regarding the mechanisms underlying DC infiltration in PBC and an epithelial neoplasm, cholangiocellular carcinoma (CCC), arising from bile ducts and the pathological significance of this phenomenon is limited. The aim of the present study was therefore to investigate the histological distribution of DCs and the mechanisms by which immature DCs infiltrate the bile ducts in PBC, compared to CCC as a neoplastic condition, by immunohistochemistry, reverse transcription polymerase chain reaction (RT-PCR) amplification and in situ hybridization.

Materials and methods
Patients and specimens

Forty-eight patients with PBC who underwent a liver biopsy to make a definitive pathological diagnosis were selected from registered case files in our department. Their median age was 58 years (range 24 to 85) and the male:female ratio was 11:37. The diagnoses were based on established criteria and were confirmed by histological review by an independent observer, which included clinical and laboratory analysis. Antimitochondrial antibody and/or antimitochondrial M2 antibody were detected in the sera of all the PBC patients by immunofluorescence. Eighty-four inflamed portal areas and hepatic lobules were selected from the biopsy specimens and the severity of the PBC was classified according to Ludwig's

histological staging method: stage I, portal hepatitis; stage II, periportal hepatitis; stage III, septal fibrosis, bridging necrosis, or both; and stage IV, cirrhosis.[22] Liver biopsy specimens from 26 patients with chronic hepatitis C (CH-C), which were obtained to make a definitive diagnosis, and normal liver specimens obtained at autopsy from three neonates were examined and compared with PBC cases. Resected tumor specimens from four patients with CCC were also examined as neoplastic bile duct tumors. The median age of CH-C patients was 59 years (range 35 to 75) and the male:female ratio was 14:9. The inflamed portal areas of the CH-C specimens were classified according to the grading and staging criteria of the International Association for the Study of Liver grades: minimal, mild, moderate, and severe activity; and stages: absent, mild, moderate, and severe fibrosis, and cirrhosis.[23]

The majority of tissue specimens were fixed in 10% formalin for 6 hours at room temperature, embedded in paraffin, and cut into 4 μm thick sections for immunohistochemistry. Liver biopsy specimens from some cases were fixed in 4% paraformaldehyde for 6 hours at 4°C to use for not only immunohistochemistry but also RT-PCR and in situ hybridization because some biopsy specimens were too small to use for independent studies.

Immunohistochemistry

After deparaffinization, the tissue sections were immersed in either 0.1% trypsin (BD Difco; BD, Franklin Lakes, NJ, USA) in 0.01 M phosphate-buffered saline (pH 7.4) with 0.1% $CaCl_2$ or 1 mM ethylenediamine tetraacetic acid solution (pH 8.0; Muto Pure Chemicals, Tokyo, Japan). These solutions were either incubated for 30 minutes at 37°C or microwaved for 20 minutes at 90°C. Endogenous peroxidase activity was blocked with methanol containing 0.3% hydrogen peroxide. When the tyramide signal amplification method was to be used, endogenous biotin activity was also blocked using the Endogenous Avidin Biotin Blocking Kit (Nichirei, Tokyo, Japan). The slides were then incubated at 4°C overnight with the relevant primary antibodies. The primary antibodies used in this study were as follows: anti S-100 protein (recognizes pan DCs; rabbit; Nichirei), CD1a (recognizes immature myeloid DCs; mouse IgG1κ; Immunotech, Marseille, France), fascin (recognizes mature DCs; mouse IgG1; DAKO, Glostrup, Denmark), DC lysosomal associated membrane protein (DC-LAMP; recognizes mature DCs; mouse IgG1; Immunotech), CD4 (mouse IgG1; Novocastra, Newcastle, UK), CD8 (mouse IgG2b; Novocastra), TIA-1 (mouse IgG1; Immunotech),

MIP-1α (goat; DAKO), MIP-1β (goat; DAKO), MIP-3α (mouse IgG1; R&D Systems, Minneapolis, MN, USA), RANTES (goat; DAKO), CCR5 (mouse IgG2b; DAKO), and CCR6 (mouse IgG2b; DAKO). The labeled streptavidin biotin peroxidase method (UltraTech HRP Streptavidin-biotin Universal Detection System; Immunotech) was used for the immunostaining of CD1a, fascin, DC-LAMP, CD4, CD8, and TIA-1, while the peroxidase-labeled dextran polymer method (EnVision+; rabbit; DAKO) was used for the immunostaining of S-100 protein. The biotinylated F(ab')$_2$ fragment of affinity isolated donkey anti-goat IgG (Jackson Immunoresearch Laboratories, West Grove, PA, USA), biotin conjugated affinity isolated goat anti-mouse IgG1 (Caltag Laboratories, Burlingame, CA, USA), and biotin-conjugated affinity isolated goat anti-mouse IgG2b (Caltag Laboratories) were used as secondary antibodies for MIP-1α, MIP-1β, MIP-3α, RANTES, CCR5, and CCR6. After using the tyramide signal amplification method for MIP-1α, MIP-1β, MIP-3α, RANTES, CCR5, and CCR6, the sections were incubated with peroxidase conjugated streptavidin (DAKO). After each step, the sections were washed with phosphate-buffered saline containing 0.1% saponin (Junsei Chemical, Tokyo, Japan). Peroxidase activity was then detected with 3,3′-diaminobenzidine (Dojin Chemicals, Kumamoto, Japan) and the sections were counterstained with hematoxylin.

Formalin fixed liver biopsy specimens from 38 patients with PBC, ten patients with CH-C and three neonates were used for the immunostaining of S-100 protein, fascin, DC-LAMP, CD4, CD8, and TIA-1. Seventy-one inflamed portal areas (including CNSDC and hepatic lobules) from the PBC specimens (stages: I, n = 15; II, n = 17; III, n = 19; IV, n = 20), 17 areas from the CH-C specimens (activity and fibrosis classes: minimal and absent, n = 1; mild and mild, n = 10; mild and severe, n = 2; moderate and mild, n = 1; moderate and moderate, n = 3), and 50 areas from the neonatal livers were selected for the counting of positive cells. Paraformaldehyde-fixed specimens from eleven patients with PBC and 17 patients with CH-C were studied for the immunostaining of MIP-1α, MIP-1β, MIP-3α, RANTES, CCR5, and CCR6. Eleven inflamed portal areas from the PBC specimens (stages: I, n = 2; II, n = 7; III, n = 2; IV, n = 0) and 17 areas from the CH-C specimens (activity and fibrosis classes: minimal and mild, n = 6; minimal and moderate, n = 3; mild and mild, n = 2; moderate and moderate, n = 1; mild and severe, n = 4; moderate and moderate, n = 1) were selected. Formalin-fixed specimens from only four patients with CCC were available for this investigation. Paired "mirror image" serial sections were used to identify cells that immunostained positively for both S-100 protein and CCR5.

Cells that were positive for each antibody (except those against chemokines and chemokine receptors) were counted in high power microscopic fields (×400) covering the epithelial layer of the bile ducts (area A), the portal areas around the bile ducts (area B), and the hepatic lobules (area C) with the aid of a computer-assisted image analyzer (ImageJ, 1.37v; Wayne Rasband, National Institutes of Health, Bethesda, MD, USA).

RNA extraction and RT-PCR amplification

Paraformaldehyde-fixed PBC and CH-C samples were used. Although mRNA is better preserved in such samples, only formalin-fixed CCC specimens were available; samples from these specimens therefore had to be used. The Pinpoint Slide RNA Isolation System II Kit (Zymo Research, Irvine, CA, USA) was used to isolate the RNA from the paraffin-embedded tissues. Ten–micrometer-thick sections were cut from the paraffin-embedded specimens and put onto a glass slide. After deparaffinization and hydration, a small amount of Pinpoint solution was spread over the selected regions. The selected areas (about 50 mm^2 each) were peeled off the dried slide. Proteinase K and RNA digestion buffer were added, and the samples were incubated for 4 hours at 55°C. RNA extraction buffer and 99.9% ethanol were then added, and the mixtures were transferred to a Zymo-Spin™ column. After washing in RNA washing buffer, prewarmed RNA elution buffer was added, the samples were centrifuged, and the RNA was eluted.

Subsequently, RT-PCR amplification was carried out using the QIAGEN OneStep RT-PCR Kit (QIAGEN, Tokyo, Japan). The extracted template mRNA was mixed with the recommended quantities of QIAGEN OneStep RT-PCR Buffer (containing 2.5 mM MgCl$_2$), dNTP Mix (containing 0.4 mM dNTP), 0.6 μM sense and antisense primers, and QIAGEN OneStep RT-PCR Enzyme Mix (containing HotStar Taq DNA polymerase).

The conditions for amplification were as follows: 40 cycles of 30 seconds at 94°C, 30 seconds at 58°C, and 30 seconds at 72°C, followed by a 10-minute extension step at 72°C.

The PCR products were resolved by electrophoresis on 1.2% or 2% agarose gels (Funakoshi, Tokyo, Japan). The bands were visualized using ethidium bromide (Bio-Rad Laboratories, Hercules, CA, USA) and the gels were photographed.

The primers used for PCR were as follows: MIP-3α (GenBank accession number D86955): 5′-TTGCTCCTGGCTGCTTTG-3′ and 5′-ACCTCCATGATGTGCAAG-3′, amplifying a 367 bp product; CCR5 (GenBank accession number X91492):

5′-GGTGGAACAAGATGGATTAT-3′ and 5′-CATGTGCACAACTCTGACTG-3′, amplifying a 1117 bp product; and CCR6 (GenBank accession number Z79784): 5′-ATTTCAGCGATGTTTTCGACTC-3′ and 5′-GGAGAAGCCTGAGGACTTGTA-3′, amplifying a 1021 bp product. RT-PCR of the porphobilinogen deaminase (*PBGD*) gene was also performed as a positive internal control to check the integrity of the mRNA isolation from each sample. The primers used to detect PBGD mRNA were 5′-TGTCTGGTAACGGCAATGCGGCTGCAAC-3′ (forward primer) and 5′-TCAATGTTGCCACCACACTGTCCGTCT-3′ (reverse primer); a 127 bp fragment was amplified.

In situ hybridization

In situ hybridization was performed on paraformaldehyde-fixed, paraffin-embedded liver biopsy specimens from PBC and CH-C patients. The oligonucleotide probes for MIP-1α and MIP-1β were constructed using a DNA synthesizer and labeled with digoxigenin (Nippon Gene Research Laboratory, Inc, Sendai, Japan). The probes used to detect MIP-1α mRNA (GenBank accession number D90144) were 5′-GCAACCAGTTCTCTGCATCACTTGCTGCTGACA-CGCCG-3′ (sense) and 5′-CGGCGTGTCAGCAGCAAGT-GATGCAGAGAACTGGTTGA-3′ (antisense). The probes used to detect MIP-1β mRNA (GenBank accession number X53682) were 5′-TCTGCGTGACTGTCCTGTCTCTCCT-CATGCTAGTAGCTGC-3′ (sense) and 5′-GGCAGCTAC-TAGCATGAGGAGAGACAGGACAGTCACGCAGA-3′ (antisense). The sections were dewaxed and rehydrated in a graded ethanol series. After treatment with 0.2 N HCl in phosphate buffered saline for 20 minutes at room temperature and digestion with 20 μg/mL proteinase-K (Sigma-Aldrich, St Louis, MO, USA) for 15 minutes at 37°C, the sections were hybridized with the sense and antisense probes overnight at 55°C. The concentration of each probe was 1 μg/mL. The sections were then washed twice with $2 \times$ SSC/60% formamide ($1 \times$ SSC contains 0.15 M sodium chloride and 0.03 M sodium citrate, pH 8.0; Junsei Chemical) for 60 minutes at 55°C, then three times with $0.5 \times$ SSC/60% formamide for 30 minutes at 55°C. The digoxigenin-labeled probes were detected using an alkaline phosphatase-conjugated rabbit antidigoxigenin antibody (DAKO) with 5-bromo-4-chloro-3-indoxyl phosphate/nitro blue tetrazolium chloride solution (DAKO) containing levamisole (DAKO) as the substrate.

Statistical analysis

Statistical analysis was performed using the Expert Stat View statistical software system (Abacus Concepts, Berkeley, CA, USA). The Mann–Whitney U test was used to compare the numbers of immunoreactive cells within the epithelial layer of the bile ducts, in the portal area around the bile ducts, and in the hepatic lobules. The same test was used to compare the numbers of immunoreactive cells among the histological staging classes. Spearman's rank correlation was used to examine the correlation between the number of S-100 protein^{+} DCs and the numbers of CD4^{+}, CD8^{+}, and TIA-1^{+} T-cells. Differences with $P < 0.05$ were considered statistically significant.

Results

Distribution of DCs in PBC

Although more S-100 protein[+] DCs were found in the epithelial layer of the bile ducts (area A) in PBC than in CH-C, there were no significant differences in the numbers of infiltrating fascin[+] and DC-LAMP[+] DCs between PBC and CH-C examined during this study (Table 1). S-100 protein[+], fascin[+], and DC-LAMP[+] DCs were very rarely found in all areas of the neonatal livers. There were also no significant differences in the numbers of fascin[+] and DC-LAMP[+] DCs in area A between the CH-C and neonatal liver samples.

In terms of sex, there was no significant difference in the number of any DC phenotypes among liver diseases, except that fewer S-100 protein[+] DCs were found in area B in female patients with CH-C than in males (data not shown).

Relationship between DC infiltration and the histological stages of PBC

In each stage of PBC except stage IV, abundant S-100 protein[+] DCs was found in area A (Table 2; Figure 1A and B). Significantly fewer S-100 protein[+] DCs were found in the portal areas around the bile ducts (area B) in the advanced stages of PBC (stages III and IV) than in the earliest stage (stage I). Furthermore, fewer infiltrating fascin[+] and DC-LAMP[+] DCs than S-100 protein[+] DCs were detected in area A. In some stages of PBC, a larger number of fascin^{+} and DC-LAMP^{+} DCs in area B were found (Figure 1C and D).

Detection of CD1a^{+} DCs in PBC and other liver diseases

Only rare CD1a^{+} DCs were found in area A in PBC, but not in any other areas of the PBC, CH-C, and neonatal liver samples (Table 1). However, CD1a^{+} DCs were observed to be infiltrating the cancer nests in CCC (Figure 2F). These cells were coincident with the S-100 protein^{+} DCs detected on the serial sections (data not shown).

Table 1 Comparison of the number of infiltrating DCs among three different areas in PBC, CH-C, and neonatal livers

Histology/type of DC	Number of positive cells/high-power field (×400), median (min, max)		
	Area A	Area B	Area C
S-100 protein[+] DCs			
PBC (n = 71)	81.4[a] (0.0, 478.1)	9.9 (1.3, 87.5)	0.3 (0.0, 2.8)
CH-C (n = 17)	0.0 (0.0, 193.4)	6.5 (0.0, 22.2)	0.3 (0.0, 1.3)
Neonatal liver (n = 50)	0.0[b] (0.0, 0.0)	0.0[c] (0.0, 5.1)	0.0[d] (0.0, 0.3)
Fascin[+] DCs			
PBC (n = 71)	0.0 (0.0, 234.9)	4.2 (0.0, 45.0)	0.3 (0.0, 1.5)
CH-C (n = 17)	0.0 (0.0, 66.2)	5.9 (0.0, 15.5)	0.3 (0.0, 0.3)
Neonatal liver (n = 50)	0.0[e] (0.0, 0.0)	0.0[f] (0.0, 0.0)	0.0[g] (0.0, 0.0)
DC-LAMP[+] DCs			
PBC (n = 71)	0.0 (0.0, 500.7)	1.3 (0.0, 62.6)	0.0 (0.0, 0.0)
CH-C (n = 17)	0.0 (0.0, 0.0)	3.2 (0.0, 30.1)	0.0 (0.0, 0.0)
Neonatal liver (n = 50)	0.0[h] (0.0, 0.0)	0.0[i] (0.0, 4.6)	0.0 (0.0, 0.0)
CD1a^{+} DCs			
PBC (n = 71)	0.0[r] (0.0, 62.7)	0.0 (0.0, 9.8)	0.0 (0.0, 0.0)
CH-C (n = 17)	0.0 (0.0, 8.5)	0.0 (0.0, 0.0)	0.0 (0.0, 0.0)
Neonatal liver (n = 50)	0.0 (0.0, 0.0)	0.0 (0.0, 0.0)	0.0 (0.0, 0.0)

Notes: Area A, epithelial layer of the bile duct; area B, portal area around the bile duct; area C, hepatic lobule. [a]The significant highest value among diseases in area A ($P < 0.01$); [b]the significant lowest value among diseases in area A ($P < 0.01$); [c]the significant lowest value among diseases in area B ($P < 0.01$); [d]the significant lowest value among diseases in area C ($P < 0.01$); [e]the significant lowest value among diseases in area A ($P < 0.01$); [f]the significant lowest value among diseases in area B ($P < 0.01$); [g]the significant lowest value among diseases in area C ($P < 0.01$); [h]the significant lower value in neonatal liver than in PBC in area A ($P < 0.05$); [i]the significant lowest value among diseases in area B ($P < 0.01$).
Abbreviations: DC, dendritic cell; PBC, primary biliary cirrhosis; CH-C, chronic hepatitis C; LAMP, lysosomal-associated membrane protein.

Distribution of T-cells in PBC

There were significant differences in the numbers of CD4^{+}, CD8^{+}, and TIA-1^{+} T-cells accumulating in areas A and B between stage IV and the other stages (Table 3). Fewer TIA-1^{+} cells were also found in area C in stage IV than in other stages.

## Relationship between DC infiltration and T-cell accumulation

In area A, there was a significant positive correlation between the number of infiltrating DCs positive for S-100 protein, fascin, and DC-LAMP and the accumulation of lymphocytes positive for CD4, CD8, and TIA-1, for CD8

Table 2 Comparison of the number of infiltrating DCs among three different areas in each histologic stage in primary biliary cirrhosis

Stage/type of DC	Number of positive cells/high-power field (×400), median (min, max)		
	Area A	Area B	Area C
S-100 protein[+] DCs			
Stage I (n = 15)	159.4 (0.0, 311.8)	14.8[a] (9.9, 73.8)	0.3 (0.0, 1.8)
Stage II (n = 17)	88.4 (0.0, 478.1)	11.0 (1.3, 87.5)	0.3 (0.0, 2.8)
Stage III (n = 19)	129.3 (14.3, 223.7)	6.6 (1.9, 67.5)	0.3 (0.0, 1.5)
Stage IV (n = 20)	7.6[b] (0.0, 93.7)	6.6 (1.7, 37.1)	0.3 (0.0, 0.8)
Fascin[+] DCs			
Stage I (n = 15)	0.0 (0.0, 234.9)	11.2 (0.0, 45.0)	0.3 (0.0, 1.5)
Stage II (n = 17)	0.0 (0.0, 126.1)	4.1 (0.0, 29.0)	0.5 (0.0, 1.0)
Stage III (n = 19)	0.0 (0.0, 158.6)	6.3 (0.0, 28.9)	0.5 (0.0, 1.0)
Stage IV (n = 20)	0.0 (0.0, 19.1)	1.3[c] (0.0, 7.9)	0.0[d] (0.0, 0.8)
DC-LAMP[+] DCs			
Stage I (n = 15)	0.0 (0.0, 500.7)	0.0 (0.0, 62.6)	0.0 (0.0, 0.0)
Stage II (n = 17)	0.0 (0.0, 466.8)	2.9 (0.0, 62.2)	0.0 (0.0, 0.0)
Stage III (n = 19)	0.0 (0.0, 71.6)	4.0 (0.0, 29.6)	0.0 (0.0, 0.0)
Stage IV (n = 20)	0.0[e] (0.0, 0.0)	0.0[f] (0.0, 2.3)	0.0 (0.0, 0.0)

Notes: Area A, epithelial layer of the bile duct; area B, portal area around the bile duct; area C, hepatic lobule. [a]the significant higher value in stage I than in stage III and IV in area B ($P < 0.05$); [b]the significant lowest value among stages in area B ($P < 0.01$); [c]The significant highest value among stages in area B ($P < 0.05$); [d]the significant lowest value among stages in area B ($P < 0.05$); [e]the significant lower value in stage IV than in stage I in area A ($P < 0.05$); [f]the significant lower value in stage IV than in stage II and III in area B ($P < 0.01$).
Abbreviations: DC, dendritic cell; LAMP, lysosomal-associated membrane protein.
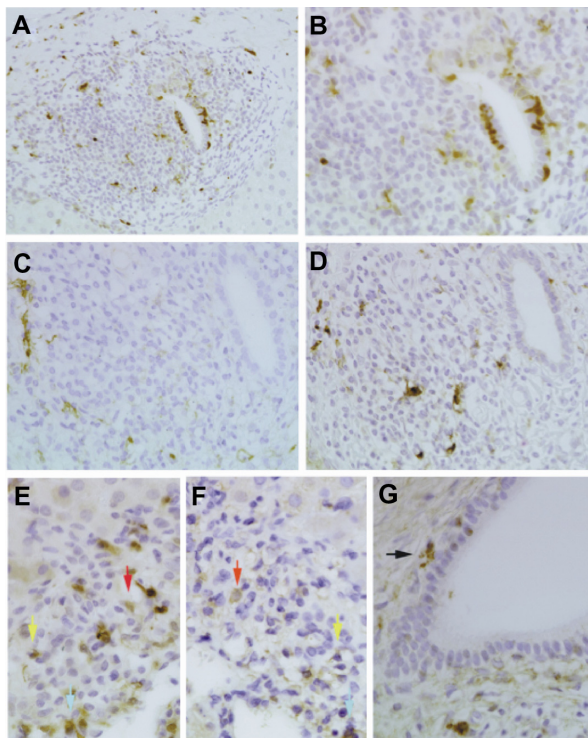
Figure 1 Immunohistochemistry demonstrating the localization of DCs in the portal area of primary biliary cirrhosis (stage II). Immunostain of S-100 protein+ (**A**, **B**, and **E**), fascin+ (**C**), DC-LAMP+ (**D**) and CCR5+ (**F** and **G**) DCs. The segments (**E**) and (**F**) are demonstrated by mirror sections. S-100 protein+, fascin+, DC-LAMP+, and CCR5+ DCs are visualized as brown. S-100 protein+ DCs infiltrate in the portal area, in particular, accumulate within the epithelium layer of the bile duct. Fascin+ and DC-LAMP+ DCs localize in the portal area around the bile duct. Less than three DCs simultaneously positive for S-100 protein (**E**) and CCR5 (**F**) in the portal area are indicated by same colored arrows, respectively. CCR5+ DCs existed in the epithelium layer of the bile duct are indicated by arrow (**G**). Counterstained with hematoxylin.
Notes: Original magnification: ×200 (**A**); ×400 (**B–G**).
Abbreviations: CCR, CC-chemokine receptor; DC, dendritic cells; LAMP, lysosomal associated membrane protein.

and TIA-1, and for TIA-1, respectively. In area B, there was a significant positive correlation between the number of infiltrating DCs positive for S-100 protein, fascin, and DC-LAMP and the accumulation of lymphocytes positive for CD4, CD8, and TIA-1, for CD4, CD8, and TIA-1, and for CD8 and TIA-1, respectively. In area C, the number of infiltrating S-100 protein+ and fascin+ DCs showed a significant positive correlation with the accumulation of TIA-1+ cells (Table 4).

Immunohistochemical expression of chemokines and their receptors

CCR5 and S-100 protein were immunostained on paired "mirror image" sections to investigate the distribution of immature DCs. In PBC, CCR5 was expressed on relatively small lymphocytes and cells with a dendritic morphology. The CCR5+ cells with a dendritic morphology corresponded

with the S-100 protein+ cells on the mirror image section (Figure 1E and F). CCR5+ cells frequently (nine of eleven samples) accumulated beneath or in damaged bile ducts (Figure 1G). By comparison, in all 17 CH-C and all four CCC samples, the CCR5+ cells were mostly small lymphocytes, and there were no cells with a dendritic morphology in area A. However, the CD1a+ cells observed in CCC corresponded with CCR6+ cells on the serial sections (Figure 2F and G). CCR6 was expressed only on small lymphocytes, which were mainly localized in the portal area in PBC and CH-C; it was never detected on cells with a dendritic morphology in this study.

In PBC, expression of MIP-1α and MIP-1β (ligands of CCR5) was detected on the epithelial cells of the bile ducts in nine of eleven samples, and was also observed on lymphocytes, mainly in the portal area (Figure 2A, C and E). In CH-C, these ligands were also expressed on lymphocytes (mainly in the portal area) but were never detected on the epithelial cells of the bile ducts. MIP-3α, a ligand of CCR6, was also restricted to small lymphocytes, again mainly in the portal area, in both PBC and CH-C; it was never found on the bile duct epithelia in either disease. Similarly, RANTES (a ligand of CCR5) was stained only on small lymphocytes that were mainly limited to the portal area in PBC and CH-C. In CCC, MIP-1α, MIP-1β, MIP-3α (Figure 2H), and RANTES were expressed on cancer nests, and there was no difference in the intensity of staining for each ligand.

Expression of chemokine and chemokine receptor mRNA

RT-PCR was performed to determine MIP-3α, CCR5, and CCR6 mRNA expression, using five PBC samples, three CH-C samples, and two CCC samples. The PBC and CH-C samples were fixed with paraformaldehyde, whereas the CCC samples were fixed with formalin. Regardless of the fixation methods and the different liver diseases, all sections expressed PBGD mRNA in almost equal amounts. MIP-3α mRNA expression was evident in four PBC and three CH-C samples, and was weak but clear in one PBC and two CCC samples. CCR5 mRNA expression was quite strong in the PBC samples, negative or faint in the CH-C samples, and weak but clear in two CCC samples. CCR6 mRNA was expressed strongly in three PBC, one CH-C, and one CCC samples, and weakly but clearly in two PBC, two CH-C, and one CCC samples (Figure 3).

In situ hybridization was performed to determine the localization of MIP-1α and MIP-1β mRNA expressed in PBC and CH-C. Eight PBC specimens (stages: I, 1; II, 6; III, 1; IV, 0) and five CH-C specimens (activity and fibrosis classes: minimal
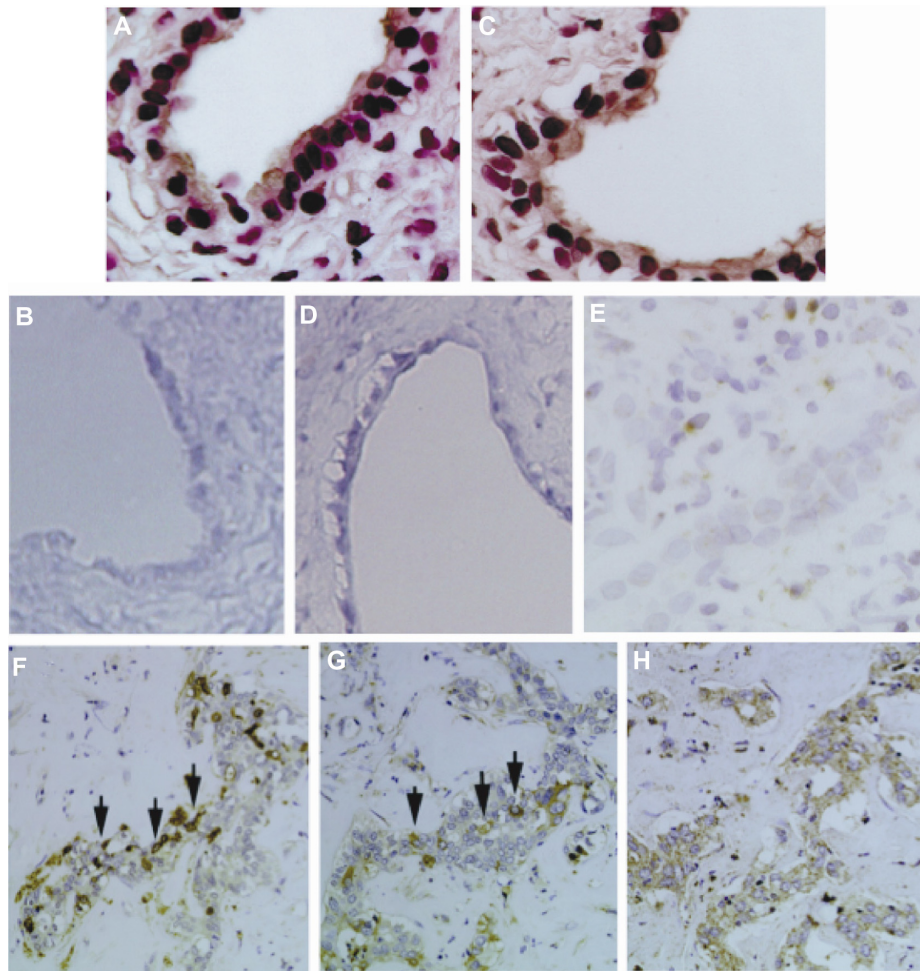
Figure 2 Immunohistochemistry and in situ hybridization demonstrating chemokine expression in primary biliary cirrhosis (stage II). MIP-1α (**A**) and MIP-1β (**C**) are immunohistochemically positive in the epithelial cells of the bile duct. In ISH, the expression of MIP-1α (**B**) and MIP-1β (**D**) mRNA are found on the epithelial cells of the bile duct. Note that MIP-3α (**E**) is immunohistochemicaly positive for lymphocytes but not the bile duct epithelial cells in the portal area. Hematoxylin is used as a counterstain in (**A**, **C**, and **E**); counterstained with hematoxylin. Immunohistochemistry demonstrating CD1a+ DCs (**F**) and CCR6+ DCs (**G**), and MIP-3α+ cancer cells (**H**) in cholangiocellular carcinoma. The segments (**F** and **G**) are demonstrating by serial sections. CD1a+ and CCR6+ DCs visualized as brown infiltrate in the cancer nests.
Notes: MIP-3α is expressed on cancer cells. Counterstained with hematoxylin. Original magnifications: ×600 (**A** and **C**); ×200 (**B**, **D**, **F–H**); ×400 (**E**).
Abbreviations: CCR, CC-chemokine receptor; DC, dendritic cells; ISH, in situ hybridization; MIP, macrophage inflammatory protein.

and absent, 2; minimal and mild, 1; mild and mild, 1; moderate and mild, 1), fixed with paraformaldehyde, were studied. Both MIP-1α and MIP-1β mRNA were expressed on the epithelial layer of the damaged bile ducts and on lymphocytes in the portal areas in PBC (six of eight samples; Figure 2B and D). The two negative samples were from stage I and II specimens, respectively. These ligands were not expressed on the epithelial layer of the bile ducts in any of the CH-C samples. The stainings were specific because no positive staining was detected when the tissues were hybridized with the sense oligonucleotide probes for MIP-1α and MIP-1β (data not shown).

Discussion

DCs are potentially important in the pathogenesis of PBC, which is characterized by the presence of antimitochondrial antibodies and progressive CNSDC of the small intrahepatic bile ducts.[24,25] Recent studies have revealed that antimitochondrial antibodies react with the E2 component of the pyruvate dehydrogenase complex E2 that binds with high intensity specifically to biliary epithelial cells.[26] However, only a few recent reports have demonstrated the localization of DCs in PBC.[10–15] In order to understand the immune response underlying progressive CNSDC of the small intrahepatic bile ducts of PBC, it is essential to investigate the localization and migration mechanisms of DCs. We have demonstrated here for the first time the precise distribution and characteristics of DCs in relation to CNSDC in PBC.

S-100+ DCs were frequently found within the epithelial layer of the bile ducts (area A) in PBC. However, the numbers of fascin+ and DC-LAMP+ mature DCs were relatively low in

Table 3 Comparison of the number of CD4^{+}, CD8^{+}, and TIA-1^{+} T lymphocytes among three different areas in each histologic stage in primary biliary cirrhosis

Stage/T lymphocytes	Number of positive cells/high-power field (×400), median (min, max)		
	Area A	Area B	Area C
CD4^{+} lymphocytes			
Stage I (n = 15)	86.4 (0.0, 726.6)	170.6 (5.1, 480.8)	2.3 (0.3, 7.0)
Stage II (n = 17)	90.0 (0.0, 753.4)	145.4 (2.4, 371.7)	1.0 (0.3, 6.3)
Stage III (n = 19)	158.6 (0.0, 590.1)	147.4 (11.0, 476.1)	1.5 (0.3, 10.3)
Stage IV (n = 20)	0.0[a] (0.0, 49.1)	70.6[b] (6.2, 155.1)	2.0 (0.0, 8.3)
CD8^{+} lymphocytes			
Stage I (n = 15)	152.7 (0.0, 764.8)	271.1 (153.4, 488.9)	5.5 (1.3, 15.3)
Stage II (n = 17)	230.9 (0.0, 579.2)	228.6 (77.9, 451.2)	4.8 (1.5, 31.8)
Stage III (n = 19)	144.6 (0.0, 508.6)	210.1 (84.2, 412.5)	6.8 (1.3, 15.0)
Stage IV (n = 20)	28.4[c] (0.0, 163.2)	55.0[d] (1.6, 164.1)	5.1 (0.3, 15.5)
TIA-1[+] lymphocytes			
Stage I (n = 15)	211.0 (0.0, 1208.8)	195.4 (48.8, 780.1)	16.8 (7.5, 39.5)
Stage II (n = 17)	150.7 (0.0, 1234.2)	532.5 (49.4, 273.4)	16.8 (2.5, 39.0)
Stage III (n = 19)	204.8 (0.0, 884.2)	143.8[e] (44.0, 278.4)	16.5 (6.5, 24.5)
Stage IV (n = 20)	0.0[f] (0.0, 69.7)	5.8[g] (1.8, 22.9)	5.8[h] (1.3, 12.3)

Notes: Area A, epithelial layer of the bile duct; area B, portal area around the bile duct; area C, hepatic lobule. [a]The significant lowest value among stages in area A ($P <$ 0.01); [b]the significant lowest value among stages in area B ($P < 0.05$); [c]the significant lowest value among stages in area A ($P < 0.01$); [d]the significant lowest value among stages in area B ($P < 0.01$); [e]the significant lower value in stage III than in stage I and II in area B ($P < 0.05$); [f]the significant lowest value among stages in area A ($P < 0.01$); [g]the significant lowest value among stages in area B ($P < 0.01$); [h]the significant lowest value among stages in area C ($P < 0.01$).

the epithelial layer of the damaged bile ducts but high in the portal area around bile ducts (area B). In contrast, both the S-100 protein[+] DCs and fascin[+] and DC-LAMP[+] mature DCs accumulated predominantly in area B in CH-C. The degree of DC infiltration was also found to be closely related to the disease stage in PBC. In stages I, II, and III, most DCs were infiltrating into the epithelial layer of the damaged bile ducts; this infiltration dropped sharply in stage IV. These findings indicate that immature DCs accumulate in the epithelial layer of the damaged bile ducts in PBC but not CH-C, demonstrating a sharp difference in the DC response to bile duct tissue between PBC and CH-C. S-100 protein[+], HLA-DR[+], or KiMlp[+] DCs and

langerin^{+} Langerhans cells were found between damaged biliary epithelial cells of septal bile ducts of livers affected by early stage (stages I and II) PBC, but were not present in ductular proliferations occurring at later stages (stages III and IV).[10,11,14,15] On the other hand, activated B7-2^{+} or CD83^{+}, BDCA-1^{+} DCs, and BDCA-2^{+} plasmacytoid DCs were preferentially observed around and between the damaged bile duct with a few located in the biliary epithelial layer, tending to decrease according to the stage of PBC.[12–15] These data suggest that DCs including Langerhans cells existing around or within biliary epithelial layers are important as periductal antigen presenting cells in PBC. Graham et al[16] proposed an attractive suggestion that

Table 4 Correlation of infiltrating DCs with T-cell subsets in primary biliary cirrhosis

Area/type of DCs	CD4	CD8	TIA-1
Area A			
S-100 protein	$r_s = 0.31$ ($P < 0.05$)	$r_s = 0.32$ ($P < 0.001$)	$r_s = 0.44$ ($P < 0.001$)
Fascin	$r_s = 0.35$	$r_s = 0.44$ ($P < 0.05$)	$r_s = 0.45$ ($P < 0.05$)
DC-LAMP	$r_s = 0.39$	$r_s = 0.41$	$r_s = 0.45$ ($P < 0.05$)
Area B			
S-100 protein	$r_s = 0.35$ ($P < 0.01$)	$r_s = 0.48$ ($P < 0.0001$)	$r_s = 0.35$ ($P < 0.01$)
Fascin	$r_s = 0.27$ ($P < 0.05$)	$r_s = 0.41$ ($P < 0.001$)	$r_s = 0.44$ ($P < 0.001$)
DC-LAMP	$r_s = 0.16$	$r_s = 0.35$ ($P < 0.01$)	$r_s = 0.33$ ($P < 0.05$)
Area C			
S-100 protein	$r_s = 0.20$	$r_s = 0.06$	$r_s = 0.33$ ($P < 0.01$)
Fascin	$r_s = 0.01$	$r_s = 0.13$	$r_s = 0.41$ ($P < 0.01$)
DC-LAMP	$r_s = 0.50$	$r_s = 0.50$	$r_s = 0.50$

Notes: Area A, epithelial layer of the bile duct; area B, portal area around the bile duct; area C, hepatic lobule.
Abbreviations: DC, dendritic cells; LAMP, lysosomal associated membrane protein; r_s, Spearman's rank correlation coefficient.
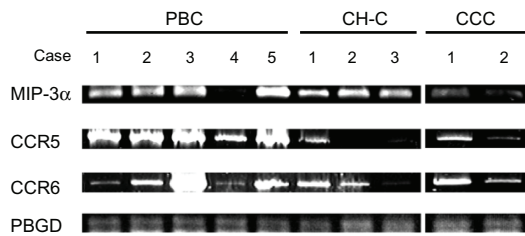
Figure 3 Expression of MIP-3α (367 bp), CCR5 (1,117 bp), and CCR6 (1,021 bp) mRNA in PBC, CH-C, and CCC by reverse transcription polymerase chain reaction.
**Note:** The PBGD (127 bp) is used as internal control.
Abbreviations: CCC, cholangiocellular carcinoma; CCR, CC-chemokine receptor; CH-C, chronic viral hepatitis C; MIP, macrophage inflammatory protein; PBC, primary biliary cirrhosis; PBGD, porphobilinogen deaminase.

the detection of a Langerhans cell infiltrate of greater than or equal to two cells by CD1a in a given bile duct on needle biopsy may be a valuable tool in the diagnosis of PBC.

Next, to clarify the correlation between DCs and T-cells, we investigated the degree of T-cell infiltration in PBC.

Abundant T-cells accumulated in the portal area (including the bile duct layer) and DCs decreased in association with advancing disease stages. The accumulation of T-cells, particularly TIA-1^{+} cells, was related to the degree of mature DC infiltration in all areas including the bile duct layer. T-cells that have been activated by mature DCs migrate into the draining lymph nodes and may be recruited to the portal area, where they may cause further injury to the bile ducts in PBC. Immature DCs probably capture any antigens in the damaged epithelial cells. Previous reports have shown that activated primed memory (CD4^{+}) and cytotoxic (CD8^{+}) T-cells were increased in PBC.[27,28] Moreover, recent reports have demonstrated that pyruvate dehydrogenase complex E2 specific CD4^{+} and CD8^{+} T-cells were identified and characterized.[29]

Several chemokines are involved in regulating the migration, activation, and maturation of DCs, and the
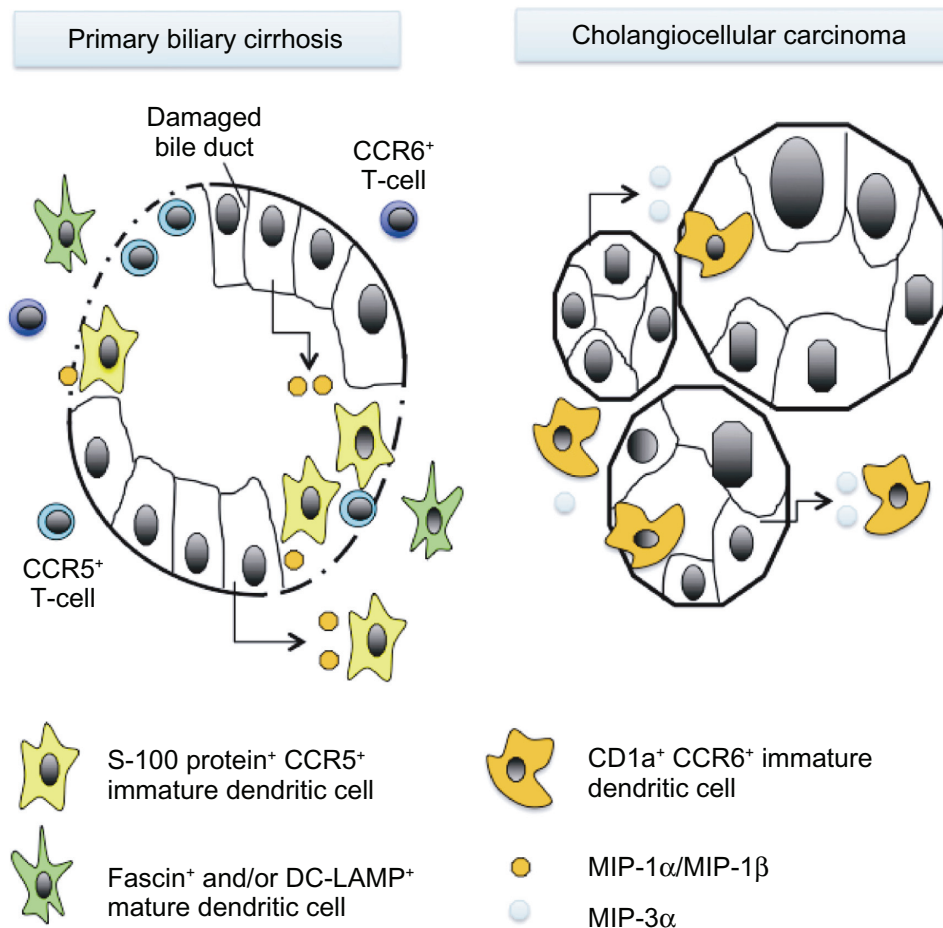
Figure 4 Scheme of the possible process of DC infiltration in PBC, compared to CCC.
Notes: The damaged bile ducts in PBC secrete MIP-1α and MIP-1β, which may be chemoattractants of S-100 protein[+] CCR5^{+} immature DCs and CCR5^{+} T-cells, forming a feature of chronic nonsuppurative destructive cholangitis of PBC. Fascin[+] and/or DC-LAMP[+] mature DCs infiltrate into the portal area, but not into the epithelial layer, of the bile ducts. In sharp contrast, neoplastic bile duct cells in CCC secrete MIP-3α, a potent chemoattractant of CD1a^{+}CCR6^{+} DCs.
Abbreviations: CCC, cholangiocellular carcinoma; CCR, CC-chemokine receptor; DC, dendritic cell; LAMP, lysosomal-associated membrane protein; MIP, macrophage inflammatory protein; PBC, primary biliary cirrhosis.

chemokine receptors expressed on immature DCs (CCR1, CCR2, CCR5, CCR6, and CXCR4) are responsible for their recruitment to inflamed tissue. Thus, CCR5^{+} immature DCs will migrate to relevant ligands, such as MIP-1α, MIP-1β, and RANTES.[4,5] In PBC, CCL2/MCP-1, CX3CL1/fractalkine, and CCL20/MIP-3α, but not CCL8/MCP-2 and CCL7/MCP-3, were expressed mainly in biliary epithelial cells, irrespective of the cause of disease.[14,15,17,20,21] The portal areas in PBC have CCL8, CCL7, CXCL10/IP-10, and CXCL9/MIG cells and chemokine receptor expressing cells (CXCR3).[17,18] Borchers et al[19] summarized that the CC chemokines CCL21 and CCL28 and the CXC chemokines CXCL9 and CXCL10 are involved in the recruitment of T lymphocytes into the portal tract in PBC and PSC, and once entering the liver, lymphocytes localize to bile duct and are retained by the combinatorial or sequential action of CXCL12, CXCL16, CX3CL1, and CCL28, and possibly CXCL9 and CXCL10. We confirmed the expression of CCR5 in PBC by immunohistochemistry. Clear expression of CCR5 mRNA was also confirmed in PBC by RT-PCR amplification, while weak expression was detected in CH-C. Furthermore, in situ hybridization demonstrated the localization of MIP-1α- and MIP-1β-mRNA on the epithelial cells of the damaged bile ducts in PBC but not in CH-C. These data imply that MIP-1α and MIP-1β expressed on bile ducts damaged by CNSDC in PBC may act as potent chemoattractants of CCR5^{+} immature DCs, although the question of whether DCs are secondary due to the destructive process of PBC bile ducts remains open.

To date, only one reported study investigated DCs infiltrating in CCC,[30] revealing that the number of CD83^{+} DCs at the invasive margin of CCC correlated significantly with the number of CD8^{+} or CD4^{+} T-cells in the cancerous region and was significantly higher in grp94^{+} cancer than in grp94^{−} cancer. Furthermore, they concluded that mature DCs are distributed predominantly at the invasive margin of cancers, and a significantly higher number of mature DCs at the invasive margin are observed in patients with grp94^{+} cancer cells. In this study, only a few CD1a^{+} DCs were found in area A of PBC, whereas CCC tissues somewhat frequently contained this type of DC. The cancer nests of CCC expressed MIP-3α and contained CCR6^{+} cells with a dendritic morphology identical to CD1a^{+} cells. Although the expression of MIP-3α-mRNA was recognized in PBC and CH-C as well as CCC by RT-PCR, immunohistochemistry indicated that it was confined to lymphocytes and was not present on the epithelial cells of the bile ducts in PBC and CH-C. Because the number of CCC specimens was low, further study will be required.

Conclusion

In summary, firstly, in PBC the damaged bile ducts expressed MIP-1α and MIP-1β, and CCR5^{+} immature DCs accumulated in and around these bile ducts (Figure 4). Secondly, there was a significant positive correlation between DC accumulation and activated T-cell infiltration within the epithelial layer of the bile ducts in PBC. Finally, the damaged but non neoplastic bile duct cells in PBC expressed MIP-1α and MIP-1β but not MIP-3α, while, in sharp contrast, neoplastic bile duct cells expressed MIP-3α, which is a potent chemoattractant of CD1a^{+} DCs. To our knowledge, this study is the first to demonstrate the significance of immature and mature DCs in and around bile duct epithelia damaged by PBC as well as CCC.

Disclosure

The authors report no conflicts of interest in this work.

References

1. Rowley DA, Fitch FW. The road to the discovery of dendritic cells, a tribute to Ralph Steinman. *Cell Immunol*. 2012;273(2):95–98.
2. Steinman RM. Decisions about dendritic cells: past, present, and future. *Annu Rev Immunol*. 2012;30:1–22.
3. Belz GT, Nutt SL. Transcriptional programming of the dendritic cell network. *Nat Rev Immunol*. 2012;12(2):101–113.
4. Sahin H, Berres ML, Wasmuth HE. Therapeutic potential of chemokine receptor antagonists for liver disease. *Expert Rev Clin Pharmacol*. 2011;4(4):503–513.
5. Blanchet X, Langer M, Weber C, Koenen RR, von Hundelshausen P. Touch of chemokines. *Front Immunol*. 2012;3:175.
6. Shute J. Glycosaminoglycan and chemokine/growth factor interactions. *Handb Exp Pharmacol*. 2012;207:307–324.
7. Behm B, Babilas P, Landthaler M, Schreml S. Cytokines, chemokines and growth factors in wound healing. *J Eur Acad Dermatol Venereol*. 2012;26(7):812–820.
8. Hamilton T, Li X, Novotny M, et al. Cell type- and stimulus-specific mechanisms for post-transcriptional control of neutrophil chemokine gene expression. *J Leukoc Biol*. 2012;91(3):377–383.
9. Murphy CT, Nally K, Shanahan F, Melgar S. Shining a light on intestinal traffic. *Clin Dev Immunol*. 2012;2012:808157.
10. Demetris AJ, Sever C, Kakizoe S, Oguma S, Starzl TE, Jaffe R. S100 protein positive dendritic cells in primary biliary cirrhosis and other chronic inflammatory liver diseases. Relevance to pathogenesis? *Am J Pathol*. 1989;134(4):741–747.
11. Rontogianni D, Gerber H, Zimmermann A. Primary biliary cirrhosis (PBC): antigen-presenting cells differ in their distribution in early and late stage PBC and involve the ductal, but not the ductular compartment. *Histol Histopathol*. 1994;9(2):211–220.
12. Kaji K, Tsuneyama K, Nakanuma Y, et al. B7-2 positive cells around interlobular bile ducts in primary biliary cirrhosis and chronic hepatitis C. *J Gastroenterol Hepatol*. 1997;12(7):507–512.
13. Tanimoto K, Akbar SM, Michitaka K, Onji M. Immunohistochemical localization of antigen presenting cells in liver from patients with primary biliary cirrhosis; highly restricted distribution of CD83-positive activated dendritic cells. *Pathol Res Pract*. 1999;195(3):157–162.
14. Harada K, Shimoda S, Ikeda H, et al. Significance of periductal Langerhans cells and biliary epithelial cell-derived macrophage inflammatory protein-3α in the pathogenesis of primary biliary cirrhosis. *Liver Int*. 2011;31(2):245–253.

15. Harada K, Nakanuma Y. Innate immunity in the pathogenesis of cholangiopathy: a recent update. *Inflamm Allergy Drug Targets*. 2012;11(6):478–483.

16. Graham RP, Smyrk TC, Zhang L. Evaluation of langerhans cell infiltrate by CD1a immunostain in liver biopsy for the diagnosis of primary biliary cirrhosis. *Am J Surg Pathol*. 2012;36(5):732–736.

17. Tsuneyama K, Harada K, Yasoshima M, et al. Monocyte chemotactic protein-1, -2, and -3 are distinctively expressed in portal tracts and granulomata in primary biliary cirrhosis: implications for pathogenesis. *J Pathol*. 2001;193(1):102–109.

18. Chuang YH, Lian ZX, Cheng CM, et al. Increased levels of chemokine receptor CXCR3 and chemokines IP-10 and MIG in patients with primary biliary cirrhosis and their first degree relatives. *J Autoimmun*. 2005;25(2):126–132.

19. Borchers AT, Shimoda S, Bowlus C, Keen CL, Gershwin ME. Lymphocyte recruitment and homing to the liver in primary biliary cirrhosis and primary sclerosing cholangitis. *Semin Immunopathol*. 2009;31(3):309–322.

20. Sasaki M, Miyakoshi M, Sato Y, Nakanuma Y. Modulation of the microenvironment by senescent biliary epithelial cells may be involved in the pathogenesis of primary biliary cirrhosis. *J Hepatol*. 2010;53(2): 318–325.

21. Sasaki M, Nakanuma Y. Novel approach to bile duct damage in primary biliary cirrhosis: participation of cellular senescence and autophagy. *Int J Hepatol*. 2012;2012:452143.

22. Nakanuma Y, Harada K. The role of the pathologist in diagnosing and grading biliary diseases. *Clin Res Hepatol Gastroenterol*. 2011;35(5): 347–352.

23. Desmet VJ, Gerber M, Hoofnagle JH, Manns M, Scheuer PJ. Classification of chronic hepatitis: diagnosis, grading and staging. *Hepatology*. 1994;19(6):1513–1520.

24. Nguyen DL, Juran BD, Lazaridis KN. Primary biliary cirrhosis. *Best Pract Res Clin Gastroenterol*. 2010;24(5):647–654.

25. Hirschfield GM. Diagnosis of primary biliary cirrhosis. *Best Pract Res Clin Gastroenterol*. 2011;25(6):701–712.

26. Joplin R, Lindsay JG, Hubscher SG, et al. Distribution of dihydrolipoamide acetyltransferases (E2) in the liver and portal lymph nodes of patients with primary biliary cirrhosis: an immunohistochemical study. *Hepatology*. 1991;14(3):442–447.

27. Kita H. Autoreactive CD8-specific T-cell response in primary biliary cirrhosis. *Hepatol Res*. 2007;37 Suppl 3:S402–S405.

28. Isse K, Harada K, Sato Y, Nakanuma Y. Characterization of biliary intra-epithelial lymphocytes at different anatomical levels of intrahepatic bile ducts under normal and pathological conditions: numbers of CD4+CD28− intra-epithelial lymphocytes are increased in primary biliary cirrhosis. *Pathol Int*. 2006;56(1):17–24.

29. Kita H, Matsumura S, He XS, et al. Quantitative and functional analysis of PDC-E2-specific autoreactive cytotoxic T lymphocytes in primary biliary cirrhosis. *J Clin Invest*. 2002;109(9):1231–1240.

30. Takagi S, Miyagawa S, Ichikawa E, et al. Dendritic cells, T-cell infiltration, and Grp94 expression in cholangiocellular carcinoma. *Hum Pathol*. 2004;35(7):881–886.